

A Control Strategy to Fast Relieve Overload in a Self-healing Smart Grid

Zaibin Jiao, *Member, IEEE*, Kun Men, and Jin Zhong, *Senior Member, IEEE*

Abstract-- Self-healing is one of the characteristics of smart grid. The self-healing functions could enable a power grid to detect the event in advance and restore the system after contingencies with minimum damages. In this paper a control strategy to fast relieve overload in the self-healing smart grid is proposed. The basic principle of the control strategy is to redistribute power flow of a contingency transmission line to other lines by using unified power flow controller (UPFC). To implement the control strategy, distributed steady-state network and wide-area measurement (WAM) -based nodal analysis are proposed and applied to redistribute power flow. The proposed WAM-based nodal analysis is carried on to relieve overload quickly and effectively while realize the control objective accurately. Moreover, grid simplification based on controllable region analysis is applied to reduce computation burden. IEEE 39-bus test system based simulation is applied to verify the proposed control strategy. The results show that the control strategy can relieve overload quickly and effectively. Thus it could be an online controller for a self-healing smart grid to deal with harmful contingencies.

Index Terms—Contingency, Emergency control, Overload, Self-healing, Smart grid, UPFC, WAMS.

I. INTRODUCTION

SMART grid has become the trend of the power grid with integration of intermittent renewable energy generations and application of latest information and communication technologies, energy storage and power electronic technologies. Self-healing is one of the seven characteristics of a smart grid as defined by DOE [1]. A self-healing smart grid identifies and reacts to system disturbances and restores the system with little or no human intervention. With the development and application of Phasor Measurement Units (PMUs) and Wide Area Measurement System (WAMS) in power grids, wide-area monitoring and control become possible for the system operator. Flexible AC Transmission System (FACTS) devices, such as UPFC, have been employed in some substations and improve the operation performance by providing pervasive control in power grid. Based on utilization of WAMS and UPFC devices, wide area control strategies and remedial action schemes have been increasingly utilized at the

transmission level to quickly prevent the spread of disturbances.

Overload is one of the most common disturbances in the power system. Usually overload itself may not lead to power system instability. However, undesired tripping of backup relays caused by long-time overloading may result in cascading failure, voltage collapse and even blackout [2]-[3]. There are many ways to relieve overload in a power grid, ranging from voltage and frequency based load shedding algorithms [4]-[15] to power flow redistribution methods through FACTS controlling [16]-[19] or corrective switching [20]-[23]. As a passive control strategy, voltage or frequency based load shedding strategy react only when emergency occurs. They do not have state prediction capability, and overload can not be relieved until detection of under-frequency or under-voltage. Moreover, load shedding will affect customer services. Power flow redistribution is preferred by utilities as an active control strategy to relieve overload without losses. Widely applied FACTS devices and communication infrastructure are the basis of this type of control strategies. The existing power flow redistribution methods employ power flow (PF) or optimal power flow (OPF) for calculations. The computation time for PF and OPF is relatively long considering the speed requirement of quickly relieving overload.

Quick response to overload contingencies and restore power grid to the normal operation condition is the major requirement of overload control strategies. The power flow redistribution strategy needs to coordinate with backup relays to avoid undesired tripping, which may result in cascading tripping, and even blackouts. Traditional power flow redistribution strategies can not fully meet the requirement of quickly relieving overload in a safe and efficient way.

In this paper, a novel control strategy is proposed for quickly relieving overload for the self-healing smart grid. UPFC is used to control bus voltages as well as active and reactive power flow. With the wide area measurement, nodal analysis is used to directly calculate the settings of UPFC parameters on the basis of superposition theorem and disturbance steady-state network. The computation time is reduced and the reaction is much quicker.

This paper is organized as follows. Section II discusses the fast overload-corrective algorithm, including the concept of disturbance steady-state network, WAM-based online interaction nodal analysis, and operation limits considered in the algorithm. Section III discusses the practical implementation of the method, including controllable regions

This work was supported by HKU Strategic Research Theme and the University Development Funding (Initiative on Clean Energy & Environment).

Z. Jiao and J. Zhong are with the Department of Electrical & Electronic Engineering of the University of Hong Kong, Hong Kong. (e-mails: zbjiao@eee.hku.hk, jzhong@eee.hku.hk).

K. Men is with China Southern Power Grid, Guangzhou, China. (e-mail: menkun@csg.cn).

and grid simplifications. A flowchart for the implementation is also discussed in the section. The proposed strategy is tested with the IEEE 39-bus system in Section IV, and simulation results are discussed and analyzed. Finally, conclusions are drawn in Section V.

II. FAST OVERLOAD CORRECTIVE ALGORITHM

A. Basic Theory

The basic theory of our proposed method is to relieve overload by superimposing a reverse current on the overloaded current of the transmission line by using superposition theorem.

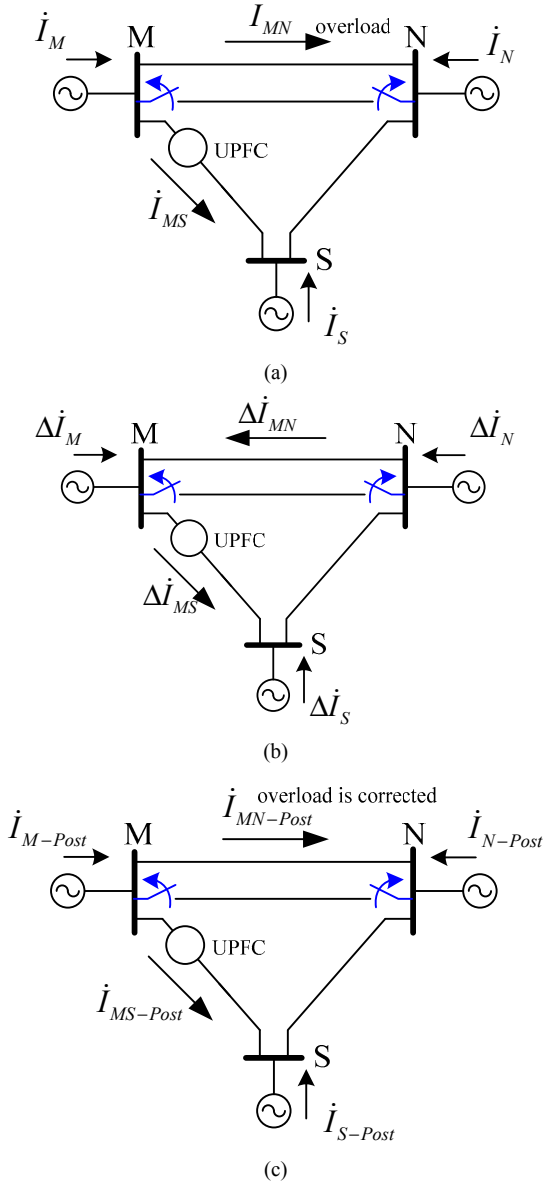


Fig. 1 Pre-disturbance network, disturbance steady state network, and post-disturbance network.

Once disturbance occurs, according to superposition theorem, the current and voltage can be considered as being composed by two components: pre-disturbance component and disturbance steady-state component. These two components can be obtained in pre-disturbance network and disturbance steady-state network, respectively, as shown in

Fig. 1. By superimposing Fig. 1(b) to Fig. 1(a), we can obtain the post-disturbance network as shown in Fig. 1(c).

Generators, loads and UPFC are modeled as current sources in this paper. The reverse current ($\Delta \dot{I}_{MN}$) can be decided according to the control objective ($\dot{I}_{MN-Post}$) and the pre-disturbance current (\dot{I}_{MN}). It is given by

$$\Delta \dot{I}_{MN} = \dot{I}_{MN-Post} - \dot{I}_{MN} \quad (1)$$

In disturbance steady-state network, the current of UPFC ($\Delta \dot{I}_{MS}$) can be calculated using nodal analysis, if $\Delta \dot{I}_{MN}$ and other current sources are known.

B. WAM-based Nodal Analysis

In practical, the injection currents of generators and loads are not known before the UPFC performs corrective action. Based on WAMS, an online interactive algorithm is proposed to decide the injection currents and parameter settings of UPFC.

All initial injections of current sources can be set to zeros in the disturbance steady-state network since the real power injected by generators and load can be specified in the power flow analysis expect for UPFC. The current and parameter settings can be calculated by nodal analysis, and followed by the corresponding actions. The injection differences of current sources before and after the UPFC corrective action are set as the initial values of current sources of the disturbance steady-state network. With the application of WAMS, the process iterates until the variation is small enough or the delay time is exceeded. During the process, the information obtained from WAMS is used as initial values for nodal analysis. The results are used to control UPFC, and the responses are employed as feedbacks to nodal analysis through WAMS. This process is called WAM-based nodal analysis in this paper.

WAM-based nodal analysis method is a totally different concept from traditional OPF or PF iteration. Corrective action is carried out in each computation step, and the overload is alleviated gradually. Usually, the overloaded transmission line can be restored during the first control action if proper reverse current is selected.

Usually, the reserve current can be set as 90% of the rating power of the transmission line.

C. Control Variable Calculation

In this paper, the injection current of UPFC is control variable. It is decided by nodal analysis which is different from the traditional iteration method.

According to nodal analysis, the bus voltage vector $\Delta \mathbf{U}$ and branch current vector $\Delta \mathbf{I}$ of disturbance steady-state network are given in (2)

$$\begin{cases} \Delta \mathbf{U} = \mathbf{Y}^{-1} \cdot \Delta \mathbf{J} \\ \Delta \mathbf{I} = \mathbf{Y}_B \cdot \mathbf{A}_A^T \cdot \Delta \mathbf{U} \end{cases} \quad (2)$$

where, \mathbf{Y} is bus admittance matrix, \mathbf{Y}_B is branch admittance matrix, \mathbf{A}_A is incidence matrix which expresses the network topology, and $\Delta \mathbf{J}$ is the bus injection current vector.

Based on (2), the reverse current $\Delta \dot{I}_{MN}$ can be expressed as

$$\Delta \dot{I}_{MN} = \dot{Y}_{MN} \cdot (\Delta \dot{U}_N - \Delta \dot{U}_M) \quad (3)$$

where, \dot{Y}_{MN} is the element of branch admittance matrix, $\Delta \dot{U}_M$ and $\Delta \dot{U}_N$ are given by

$$\Delta \dot{U}_M = \dot{Z}_{MM} \cdot (-\Delta \dot{I}_{MS} + \Delta \dot{I}_M) + \dot{Z}_{MS} \cdot (\Delta \dot{I}_{MS} + \Delta \dot{I}_S) + \dot{Z}_{MN} \cdot \Delta \dot{I}_N \quad (4)$$

$$\Delta \dot{U}_N = \dot{Z}_{NN} \cdot (-\Delta \dot{I}_{NS} + \Delta \dot{I}_N) + \dot{Z}_{NS} \cdot (\Delta \dot{I}_{MS} + \Delta \dot{I}_S) + \dot{Z}_{MN} \cdot \Delta \dot{I}_M \quad (5)$$

where, \dot{Z}_{MM} , \dot{Z}_{MN} , \dot{Z}_{NN} , \dot{Z}_{MS} and \dot{Z}_{NS} are the elements of matrix \mathbf{Y}^{-1} .

The injection current of UPFC can be derived from (3) - (5). It is expressed as follows

$$\Delta \dot{I}_{MS} = \frac{\Delta \dot{U}'_{MN} - \Delta \dot{U}'_N + \Delta \dot{U}'_M}{\dot{Z}_{NS} - \dot{Z}_{MN} - \dot{Z}_{MS} + \dot{Z}_{MM}} \quad (6)$$

where

$$\Delta \dot{U}'_{MN} = \frac{\Delta \dot{I}_{MN}}{\dot{Y}_{MN}} \quad (7)$$

$$\Delta \dot{U}'_N = \dot{Z}_{MN} \Delta \dot{I}_M + \dot{Z}_{NS} \Delta \dot{I}_S + \dot{Z}_{NN} \Delta \dot{I}_N \quad (8)$$

$$\Delta \dot{U}'_M = \dot{Z}_{MM} \Delta \dot{I}_M + \dot{Z}_{MS} \Delta \dot{I}_S + \dot{Z}_{MN} \Delta \dot{I}_N \quad (9)$$

Considering bus voltage violation in emergency conditions, the injection current of UPFC can be also derived from (4) or (5) based on nodal analysis. It is shown as follows

$$\Delta \dot{I}_{MS} = \frac{(\dot{U}_{M-Post} - \dot{U}_M) - \Delta \dot{U}'_N}{\dot{Z}_{NS} - \dot{Z}_{MN}} \quad (10)$$

where, \dot{U}_{M-Post} is the control objective, which is a constant value that satisfies voltage constraints of power systems.

D. Operation Constraints

Operation limits need to be considered in the proposed control strategy to avoid the violations of currents and voltages caused by UPFC injection current. The injection currents of UPFCs need to satisfy regular power flows as well as voltage limits. Besides, the operation constraints of the UPFC should also be considered in the control strategy.

The inequality constraints can be expressed as follows.

$$I_{injection} < I_{injection.max} \quad (11)$$

where, $I_{injection.max}$ is the maximum allowed injection current according to the line load rating and the bus voltage limit.

Assume a UPFC is placed between bus i and bus j , the limit of its injection current is described as follows:

$$I_{injection.max} = \min\{I_{load}, I_{voltage}\} \quad (12)$$

where, I_{load} is the injected current limit according to line power rating, $I_{voltage}$ is the injected current limit according to bus voltage.

For a specific transmission line, the injection current limit

of UPFC can be calculated by power ratings. According to (6), the injection current limit can be shown as follows

$$I_{load} = \min_{m,n \in N} \left\{ \frac{\Delta \dot{U}'_{mn} - \Delta \dot{U}'_n + \Delta \dot{U}'_m}{\dot{Z}_{ni} - \dot{Z}_{nj} - \dot{Z}_{mi} + \dot{Z}_{mj}} \right\} \quad (13)$$

where, N is the set of nodes, $\Delta \dot{U}'_{mn} = \frac{i_{mn} - i_{mn-max}}{\dot{Y}_{mn}}$, i_{mn-max} is the

power rating of branch mn , i_{mn} is the overloaded current.

The injection current limits of UPFC are also needed to be calculated by the upper and lower limits of bus voltages according to (10).

Moreover, the operation constraints of the UPFC are considered in the control strategy. As discussed in [24] and [25], a UPFC has six operational constraints: maximum real power exchanged between two VSCs; MVA rating of shunt VSC; MVA rating of series VSC; minimum voltage magnitude of shunt VSC; maximum voltage magnitude of series VSC and maximum voltage magnitude of shunt VSC.

III. METHOD AND IMPLEMENTATION

A. Grid Simplification

UPFC is commonly used to control power flow in the transmission network. However, this is not suitable for the radial lines at the end of a network. The controllable region should be identified before UPFC control is applied. Based on the IEEE 39-bus system, as shown in Fig. 2, we will identify the UPFC controllable region and find the equivalent circuit by using grid simplification method.

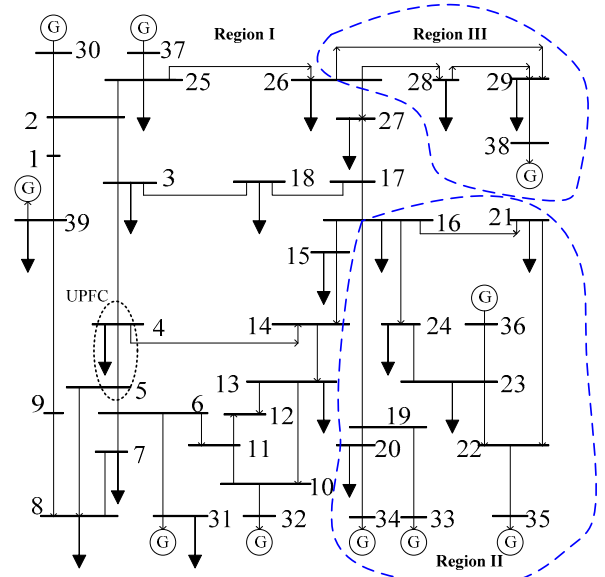


Fig. 2 Ten-generator 39-bus New England test system

In Fig. 2, we find that two regions are not controllable by UPFC, region II and region III. Region II include bus 19, 20, 21, 22, 23, 24, 33, 34, 35 and 36, Region III include bus 28, 29 and 38. The rest of buses are Region I, which is controllable as shown in Fig. 2.

Region II and III are UPFC uncontrollable because there is not path for real power flow if a real power is injected at bus 16 and bus 26, individually. However, there are ground return

path for injected reactive power in disturbance steady-state network. Reactive power distributions in Region II and III are affected by the injection in Region I. This influence can be ignored due to very small magnitude of reactive power. Similarly, buses 30, 31, 32 and 37 can be simplified by connecting generators to buses 2, 6, 10 and 25 as shown in Fig. 2. The final simplified grid is shown in Fig. 3, which is equivalent to Fig. 2 from the aspect of UPFC control. The original 10-generators and 39-buses system is represented by a 7-generators and 22-buses system.

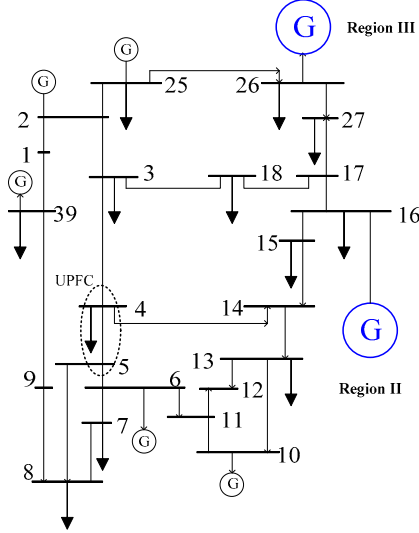


Fig. 3 Simplified ten-generator 39-bus New England test system

B. Implementation

The control strategy is implemented by using WAM-based nodal analysis.

Once an overload occurs, by setting all generator and load injection currents to zeros, control variable can be calculated through disturbance steady-state network to directly correct the overload and voltage violation. If the contingency is not completely relieved by this action, the overload is at least reduced, which will extend the operation time of backup relays due to inverse-time characteristics. In case the overload is completely corrected while the control objective is not reached, the WAM-based nodal analysis will be performed iteratively until the control objective is reached or being interrupted by the system operator. The process can also be stopped due to the restriction of the UPFC capacity limits.

The flowchart of the proposed control strategy is provided in Fig. 4.

The blocks marked by ①-④ in Fig. 4 are the steps need to use WAMS. The block marked by ⑤ is the step need human-machine interaction.

In ①, the relay pickup signals obtained from WAMS are used to trigger the control strategy. In ②, the network topology is adjusted according to the status of circuit breakers, which are also from WAMS. The controllable region is identified based on the network topology. In ③, the reset signals come from WAMS are used to cease the control strategy. The most important is that injection currents of generators and loads are from WAMS in ④.

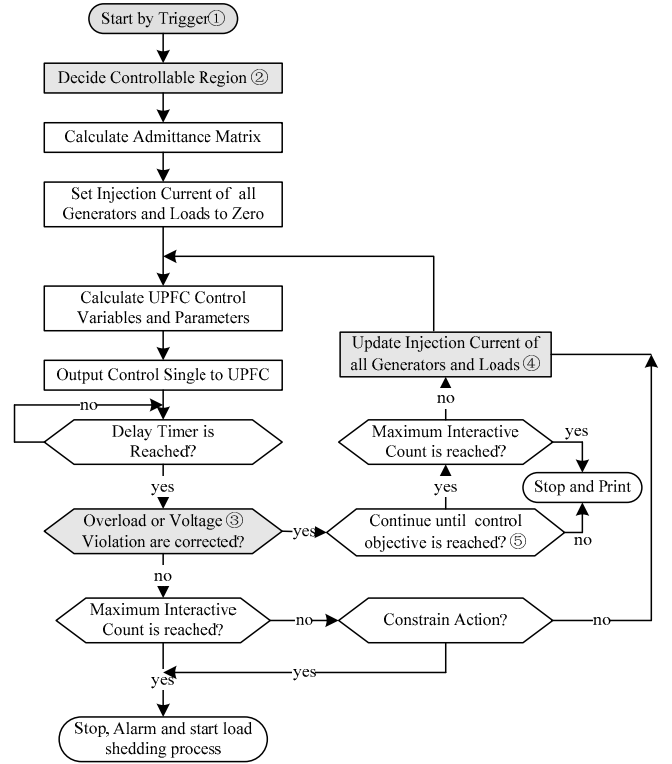


Fig. 4 Flowchart of the proposed control strategy

IV. CASE STUDY

In order to verify the proposed corrective control strategy, IEEE 39-bus system is used for the case study.

The one-line diagram of test system is shown in Fig. 2. In the case study, the AC power flow analysis before and after the control process is performed using software DIgSILENT/PowerFactory.

The UPFC is placed in branch 4-5. The real power 50 MW is injected to bus 5 and the reactive power 12.5 Mvar are injected to both bus 4 and bus 5.

Assume a tripping of branch 16-17 results in a overload of branch 4-14. The controllable region and grid simplification method is verified firstly.

Powers injected from Region II and III after tripping branch 16-17 are shown in Table I.

TABLE I
POWER INJECTION FROM GROUP II AND III AFTER BRANCH 16-17 TRIPPING

| BUS | Power (Before Disturbance) | Power (After Disturbance) | Power Injection |
|------------|--------------------------------|-------------------------------|------------------------------|
| 16 (16-19) | P: 456.83 MW Q: 67.03 Mvar | P: 456.77 MW Q: 83.64 Mvar | P: -0.06 MW Q: 16.61 Mvar |
| 16 (16-24) | P: 43.43 MW Q: 98.66 Mvar | P: 43.42 MW Q: 106.15 Mvar | P: -0.01 MW Q: 7.49 Mvar |
| 16 (16-21) | P: 330.27 MW Q: -14.04 Mvar | P: 330.22 MW Q: -2.49 Mvar | P: -0.05 MW Q: 11.55 Mvar |
| 26 (26-28) | P: 143.47 MW Q: 26.34 Mvar | P: 143.48 MW Q: 26.99 Mvar | P: 0.01 MW Q: 0.65 Mvar |
| 26 (26-29) | P: 192.72 MW Q: 30.02 Mvar | P: 192.71 MW Q: 30.66 Mvar | P: -0.01 MW Q: 0.64 Mvar |

For the bus 16 and 26, the real powers injected from Region II and III are quite constant after disturbances, while the reactive power injections are changed significantly. The results verified the analysis of controllable region and supported the grid simplification method discussed in above.

The proposed control strategy is performed in the controllable region which only involves 7 generators and 22 buses.

Contingency analysis of branch 4-14 is shown in Table II.

TABLE II
CONTINGENCY ANALYSIS OF BRANCH 4-14

| Overloaded Line | Line Flow | Line Rating | Amount of Overload |
|-----------------|---|-------------|--------------------|
| Line 4-14 | P: 594.74MW Q: 4.46Mvar S=594.76MVA | 500MVA | 94.76MVA |

From Table II, the power flow of branch 4-14 is 594.76MVA after tripping the branch 16-17. The amount of overload is 94.76 MVA, which is needed to relieve by UPFC.

In this case, the control objective is set as 90% of line rating. And the acceptable error is set to be 1%. The proposed control strategy is tested in the whole grid and in Region I. Based on the flowchart shown in Fig. 4, all injection currents of generators and loads are set to zeros in the first iteration to calculate the control variable. The test results are shown in Table III - VI and Table VII - X.

Table III shows the control variable calculated by WAM-based nodal analysis. Table IV shows the control results from DIGSILENT simulator.

In the first iteration process of the proposed control strategy, the overload is alleviated but the control objective is not reached as shown in Table IV. The errors are produced from the injection currents of generators and loads, caused by variation of voltage and reactive power. Magnitudes of the injection currents are small enough and could be ignored. Table IV also shows that overload is not increased by corrective action of UPFC even if all injection currents of generators and loads are set to zeros.

TABLE III
UPFC CONTROL VARIABLE---CURRENT AND POWER INJECTION

| Injection Bus | Addition Power (Real Power) | Addition Power (Reactive Power) | Addition Power |
|---------------|-----------------------------|---------------------------------|----------------|
| Bus 4 | -171.06MW | 45.78Mvar | 177.08MVA |
| Bus 5 | 173.85MW | -46.53Mvar | 179.97MVA |
| Injection Bus | Total Power (Real Power) | Total Power (Reactive Power) | Total Power |
| Bus 4 | -121.06MW | 33.28 Mvar | 125.55 MVA |
| Bus 5 | 123.85MW | -59.03 Mvar | 137.20 MVA |
| Injection Bus | Injection Current | | |
| Bus 4 | -0.9929+j0.2647 kA | | |
| Bus 5 | 0.9929-j0.2647 kA | | |

TABLE IV
OBJECTIVE, RESULT AND ERROR IN THE FIRST ITERATION

| Branch | Objective | Result | error(%) |
|-----------|----------------|------------|-----------------|
| Line 4-14 | Real Power | 449.98MW | 458.48MW / |
| | Reactive Power | 3.3744MVar | 44.43MVar / |
| | Power | 450MVA | 460.63MVA 2.36% |

Operators can stop the process of control strategy according to the results of the first iteration because overload has been alleviated and the system is restored to another normal operation conditions. However, they can also continue the process of control strategy to redistribute the power flow because the error is 2.36%, which is larger than the control objective (1%).

In the second iteration, the injection currents of generators and loads are calculated by using data from WAMS according to the block marked ④ in Fig.4. The control results are shown in Table V - VI. It is seen from Table V that the error is only

0.11%, and the control objective is reached.

TABLE V
UPFC CONTROL VARIABLE---CURRENT AND POWER INJECTION

| Injection Bus | Addition Power (Real Power) | Addition Power (Reactive Power) | Addition Power |
|---------------|-----------------------------|---------------------------------|----------------|
| Bus 4 | -182.30MW | 11.55Mvar | 182.67MVA |
| Bus 5 | 183.55MW | -11.63Mvar | 183.92MVA |
| Injection Bus | Total Power (Real Power) | Total Power (Reactive Power) | Total Power |
| Bus 4 | -132.30MW | -0.95 Mvar | 132.30 MVA |
| Bus 5 | 133.55MW | -24.13 Mvar | 135.71 MVA |
| Injection Bus | Injection Current | | |
| Bus 4 | -1.0518+j0.0696 kA | | |
| Bus 5 | 1.0518-j0.0696 kA | | |

TABLE VI
OBJECTIVE, RESULT AND ERROR IN THE SECOND ITERATION

| Branch | Objective | Result | error(%) |
|-----------|----------------|------------|-----------------|
| Line 4-14 | Real Power | 449.98MW | 449.96MW / |
| | Reactive Power | 3.3744MVar | 22.08MVar / |
| | Power | 450MVA | 450.50MVA 0.11% |

From the simulation results, we can conclude the overload is alleviated in the first iteration if the control objective is set with sufficient margin. However, a large margin will result new overloads and voltage violations. A proper control objective is very important to fast relieve overload in a safe way. 90% of transmission line rating is suggested as control objective in the proposed control strategy.

In order to benchmark the results from the whole grid, proposed control strategy is also performed in the simplified grid and the corresponding results are shown in Table VII - X.

Table VII and VIII show the results of the first iteration of controllable region.

TABLE VII
UPFC CONTROL VARIABLE---CURRENT AND POWER INJECTION

| Injection Bus | Addition Power (Real Power) | Addition Power (Reactive Power) | Addition Power |
|---------------|-----------------------------|---------------------------------|----------------|
| Bus 4 | -171.86MW | 46.00Mvar | 177.91MVA |
| Bus 5 | 174.66MW | -46.75Mvar | 180.81MVA |
| Injection Bus | Total Power (Real Power) | Total Power (Reactive Power) | Total Power |
| Bus 4 | -121.86MW | 33.50 Mvar | 126.38 MVA |
| Bus 5 | 124.66MW | -59.25 Mvar | 138.02 MVA |
| Injection Bus | Injection Current | | |
| Bus 4 | -0.9974+j0.2664 kA | | |
| Bus 5 | 0.9974-j0.2664 kA | | |

TABLE VIII
OBJECTIVE, RESULT AND ERROR IN THE FIRST ITERATION

| Branch | Objective | Result | error(%) |
|-----------|----------------|------------|-----------------|
| Line 4-14 | Real Power | 449.98MW | 457.85MW / |
| | Reactive Power | 3.3744MVar | 44.61MVar / |
| | Power | 450MVA | 460.02MVA 2.23% |

Table IX and X show the results of the second iteration of the controllable region.

TABLE IX
UPFC CONTROL VARIABLE---CURRENT AND POWER INJECTION

| Injection Bus | Addition Power (Real Power) | Addition Power (Reactive Power) | Addition Power |
|---------------|-----------------------------|---------------------------------|----------------|
| Bus 4 | -182.97MW | 26.07Mvar | 184.82MVA |
| Bus 5 | 184.92MW | -26.35Mvar | 186.79MVA |
| Injection Bus | Total Power (Real Power) | Total Power (Reactive Power) | Total Power |
| Bus 4 | -132.97MW | 13.57 Mvar | 133.66 MVA |
| Bus 5 | 134.92MW | -38.85 Mvar | 137.97 MVA |
| Injection Bus | Injection Current | | |
| Bus 4 | -1.0581+j0.1516 kA | | |
| Bus 5 | 1.0581-j0.1516 kA | | |

TABLE X
OBJECTIVE, RESULT AND ERROR IN THE SECOND ITERATION

| Branch | Objective | Result | error(%) | |
|-----------|----------------|------------|-----------|-------|
| Line 4-14 | Real Power | 449.98MW | 449.25MW | / |
| | Reactive Power | 3.3744MVar | 31.81MVar | / |
| | Power | 450MVA | 450.37MVA | 0.08% |

Comparing the results obtained in the controllable region to those in the whole grid, we can conclude that there are no any significant differences. Errors are both very small and can be ignored in practical applications. Performing proposed control strategy in controllable region, Region I in this case, can effectively save computing time and then relieve overload faster due to less generators and loads.

V. CONCLUSION

Redistributing power flow by UPFC in contingencies is an advanced control method to relieve overload and will be accepted by power utilities as the load shedding can be avoided. Based on disturbance steady-state network and online interactive algorithm, the proposed control strategy can fast relieve overload and can meet the requirement of self-healing smart grid. The proposed control strategy can be concluded as follows:

(1) Based on disturbance steady-state network and online interactive algorithm with wide area measurements, the injection current of UPFC can be calculated directly in the control strategy instead of using iteration and optimization.

(2) Control variables are calculated in a controllable region whose scale is smaller than that of the whole grid. The order of the admittance matrixes of bus and branch are both reduced significantly and the computation burden is reduced.

(3) Overload can be corrected by the first control action with a proper control objective setting. The power grid can be restored to another normal operation condition as soon as possible. The control objective can be achieved by using wide area measurements.

Case study and simulation results on an IEEE 39-bus system show that the proposed control strategy can fast relieve overload and can meet the requirement of self-healing smart grid.

VI. REFERENCES

- [1] "The NETL Modern Grid Initiative: A System View of the Modern Grid Version 2.0, Conducted by the National Energy Technology Laboratory for the U.S. Department of Energy Office of Electricity Delivery and Energy Reliability, January 2007" [Online]. Available: http://www.netl.doe.gov/smartgrid/referenceshelf/whitepapers/ASystemsViewoftheModernGrid_Final_v2_0.pdf
- [2] K. J. Yunus, G. Pinares, L. A. Tuan and L. Bertling, "A combined zone-3 relay blocking and sensitivity-based load shedding for voltage collapse prevention," in *Proc. 2010 Innovative Smart Grid Technologies Conference Europe (ISGT Europe)*, 2010 IEEE PES, pp. 1-8.
- [3] T. S. Bi, H. M. Xu, S. F. Huang and Q. X. Yang, "Flow transferring identification algorithm with consideration of transient period," in *Proc. 2009 Power & Energy Society General Meeting*, 2009. PES '09. IEEE, pp. 1-5.
- [4] A. A. Girgis and S. Mathure, "Application of active power sensitivity to frequency and voltage variations on load shedding," *Electric Power Systems Research*, vol.80, pp. 306-310, 2010.
- [5] C. W. Taylor, "Concepts of Undervoltage Load Shedding for Voltage Stability," *IEEE Tran. Power Delivery*, vol. 7, no. 2, pp. 480-488, Apr. 1992

- [6] P. M. Anderson and M. Mirheydar, "An adaptive method for setting underfrequency load shedding relays," *IEEE Tran. Power Systems*, vol.7, pp. 647-655, 1992.
- [7] Y. Haibo, V. Vittal and Y. Zhong, "Self-healing in power systems: an approach using islanding and rate of frequency decline-based load shedding," *IEEE Tran. Power Systems*, vol.18, pp. 174-181, 2003.
- [8] A. Saffarian and M. Sanaye-Pasand, "Enhancement of Power System Stability Using Adaptive Combinational Load Shedding Methods," *IEEE Tran. Power Systems*, vol.26, pp. 1010-1020, 2011.
- [9] A. P. Ghaleh, M. Sanaye-Pasand and A. Saffarian, "Power system stability enhancement using a new combinational load-shedding algorithm," *Generation, Transmission & Distribution, IET*, vol.5, pp. 551-560, 2011.
- [10] L. D. Arya, V. S. Pande and D. P. Kothari, "A technique for load-shedding based on voltage stability consideration," *International Journal of Electrical Power & Energy Systems*, vol.27, pp. 506-517, 2005.
- [11] M. El Arini, "Optimal dynamic load shedding policy for generation load imbalances including characteristics of loads," *International Journal of Energy Research*, vol.23, pp. 79-89, 1999.
- [12] M. A. Mostafa, M. E. El-Hawary, M. M. Mansour, K. M. El-Nagar and A. M. El-Arabaty, "Optimal dynamic load shedding using a Newton based dynamic algorithm," *Electric Power Systems Research*, vol.34, pp. 157-163, 1995.
- [13] H. Ying-Yi and W. Shih-Fan, "Multiobjective Underfrequency Load Shedding in an Autonomous System Using Hierarchical Genetic Algorithms," *Power Delivery, IEEE Transactions on*, vol.25, pp. 1355-1362, 2010.
- [14] D. Novosel and R. L. King, "Using artificial neural networks for load shedding to alleviate overloaded lines," *IEEE Tran. on Power Delivery*, vol.9, pp. 425-433, 1994.
- [15] S. K. Tso, T. X. Zhu, Q. Y. Zeng and K. L. Lo, "Evaluation of load shedding to prevent dynamic voltage instability based on extended fuzzy reasoning," *Generation, Transmission and Distribution, IEE Proceedings-*, vol.144, pp. 81-86, 1997.
- [16] W. Shao and V. Vittal, "LP-based OPF for corrective FACTS control to relieve overloads and voltage violations," *IEEE Tran. Power Systems*, vol.21, pp. 1832-1839, 2006.
- [17] L. Lenoir, I. Kamwa and L. A. Dessaint, "Overload Alleviation With Preventive-Corrective Static Security Using Fuzzy Logic," *IEEE Tran. Power Systems*, vol.24, pp. 134-145, 2009.
- [18] A. M. Haddadi and A. Kazemi, "Optimal power flow control by rotary power flow controller," *Advances in Electrical and Computer Engineering*, vol.11, pp. 79-86, 2011.
- [19] R. Zarate-Mihano, A. J. Conejo and F. Milano, "OPF-based security redispatching including FACTS devices," *Generation, Transmission & Distribution, IET*, vol.2, pp. 821-833, 2008.
- [20] S. Wei and V. Vittal, "Corrective switching algorithm for relieving overloads and voltage violations," *IEEE Tran. Power Systems*, vol.20, pp. 1877-1885, 2005.
- [21] A. A. Abou EL Ela and S. R. Spea, "Optimal corrective actions for power systems using multi-objective genetic algorithms," *Electric Power Systems Research*, vol.79, pp. 722-733, 2009.
- [22] K. W. Hedman, R. P. O'Neill, E. B. Fisher and S. S. Oren, "Optimal Transmission Switching With Contingency Analysis," *IEEE Tran. on Power Systems*, vol.24, pp. 1577-1586, 2009.
- [23] A. Khodaei and M. Shahidehpour, "Transmission switching in security-constrained unit commitment," *IEEE Trans. Power Systems*, vol.25, pp. 1937-1945, 2010.
- [24] Y. H. Song and A. T. Johns, *Flexible AC Transmission Systems (FACTS)*. London, U.K.: Inst. Elect. Eng., 1999.
- [25] J. Bian, D. G. Ramey, and R. J. Nelson et al., "A Study of equipment sizes and constrains for a unified power flow controller," *IEEE Tran. Power Del.*, vol.12, no.3, pp. 1385-1391, 1997.

VII. BIOGRAPHIES

Zaibin Jiao (M'10) received his B.Sc. and M. Sc degree from Southwest Jiaotong University, Chengdu, China and the Ph.D. degree from Xi'an Jiaotong University, Xi'an, China. He joined Xi'an Jiaotong University in 2008. Currently, he works as a Lecturer at the School of Electrical Engineering. From 2011, he starts to visit the University of Hong Kong as a Post Doctoral Fellow. His areas of interest are power system protection and smart grid.

Kun Men received his B.Sc. degree from Xi'an Jiaotong University, Xi'an, China, the M. Sc. degree from Tsinghua University and the Ph.D. degree from Texas A&M University. He used to be a Senior Engineer at Siemens EMEA in Minneapolis. Currently he is a Lead Engineer at China Southern Power Grid Co. His areas of interest are power system stability analysis, power system control, and power system simulation.

Jin Zhong (M'05, SM'10) received her B.Sc. degree from Tsinghua University, Beijing, China, the M. Sc. degree from China Electric Power Research Institute and the Ph.D. degree from Chalmers University of Technology, Gothenburg, Sweden, in 2003. At present, she is an Associate Professor in the Department of Electrical and Electronic Engineering, the University of Hong Kong. Her areas of interest are power system operation, electricity sector deregulation, ancillary service pricing, and smart grid.